The Effect of Malnutrition on Norovirus Infection

Danielle Hickman,[a] Melissa K. Jones,[a] Shu Zhu,[a] Ericka Kirkpatrick,[a] David A. Ostrov,[b] Xiaoyu Wang,[c] Maria Ukhanova,[d] Yijun Sun,[c] Volker Mai,[d] Marco Salemi,[e] Stephanie M. Karst[a]

College of Medicine, Department of Molecular Genetics and Microbiology, Emerging Pathogens Institute, University of Florida, Gainesville, Florida, USA[a]; College of Medicine, Department of Pathology, Immunology, and Laboratory Medicine, Center for Neurogenetics, University of Florida, Gainesville, Florida, USA[b]; Departments of Microbiology and Immunology, Computer Science and Engineering, and Biostatistics, State University of New York at Buffalo, Buffalo, New York, USA[c]; College of Public Health and Health Professions & College of Medicine, Department of Epidemiology, Emerging Pathogens Institute, University of Florida, Gainesville, Florida, USA[d]; Department of Pathology, Immunology, and Laboratory Medicine, Emerging Pathogens Institute, College of Medicine, University of Florida, Gainesville, Florida, USA[e]

ABSTRACT **Human noroviruses are the primary cause of severe childhood diarrhea in the United States, and they are of particular clinical importance in pediatric populations in the developing world. A major contributing factor to the general increased severity of infectious diseases in these regions is malnutrition—nutritional status shapes host immune responses and the composition of the host intestinal microbiota, both of which can influence the outcome of pathogenic infections. In terms of enteric norovirus infections, mucosal immunity and intestinal microbes are likely to contribute to the infection outcome in substantial ways. We probed these interactions using a murine model of malnutrition and murine norovirus infection. Our results reveal that malnutrition is associated with more severe norovirus infections as defined by weight loss, impaired control of norovirus infections, reduced antiviral antibody responses, loss of protective immunity, and enhanced viral evolution. Moreover, the microbiota is dramatically altered by malnutrition. Interestingly, murine norovirus infection also causes changes in the host microbial composition within the intestine but only in healthy mice. In fact, the infection-associated microbiota resembles the malnutrition-associated microbiota. Collectively, these findings represent an extensive characterization of a new malnutrition model of norovirus infection that will ultimately facilitate elucidation of the nutritionally regulated host parameters that predispose to more severe infections and impaired memory immune responses. In a broad sense, this model may provide insight into the reduced efficacy of oral vaccines in malnourished hosts and the potential for malnourished individuals to act as reservoirs of emergent virus strains.**

IMPORTANCE **Malnourished children in developing countries are susceptible to more severe infections than their healthy counterparts, in particular enteric infections that cause diarrhea. In order to probe the effects of malnutrition on an enteric infection in a well-controlled system devoid of other environmental and genetic variability, we studied norovirus infection in a mouse model. We have revealed that malnourished mice develop more severe norovirus infections and they fail to mount effective memory immunity to a secondary challenge. This is of particular importance because malnourished children generally mount less effective immune responses to oral vaccines, and we can now use our new model system to probe the immunological basis of this impairment. We have also determined that noroviruses evolve more readily in the face of malnutrition. Finally, both norovirus infection and malnutrition independently alter the composition of the intestinal microbiota in substantial and overlapping ways.**

Received 28 November 2013 **Accepted** 4 February 2014 **Published** 4 March 2014

Citation Hickman D, Jones MK, Zhu S, Kirkpatrick E, Ostrov DA, Wang X, Ukhanova M, Sun Y, Mai V, Salemi M, Karst SM. 2014. The effect of malnutrition on norovirus infection. mBio 5(2):e01032-13. doi:10.1128/mBio.01032-13.

Editor Vincent Racaniello, Columbia University College of Physicians & Surgeons

Address correspondence to Stephanie M. Karst, skarst@ufl.edu.

Human noroviruses (HuNoVs) are a significant cause of gastroenteritis outbreaks across the globe, implicated in more than 95% of nonbacterial outbreaks. These highly infectious and ubiquitous plus-strand RNA viruses spread from person to person and via fecal-oral contamination and symptomatically infect people of all ages. In the United States, they have been recognized as the leading cause of severe childhood diarrhea since the introduction of efficacious rotavirus vaccines (1, 2). Numerous viruses are known to cause more severe infections in malnourished hosts (3, 4). Thus, it is highly likely that HuNoV infections are even more devastating in developing countries, where people commonly lack access to basic medical care, sanitary water, and a sufficient diet. Indeed, one survey of the association of HuNoVs with severe diarrhea concluded that HuNoVs likely cause more than 1 million hospitalizations and 200,000 deaths annually in children in the developing world (5). Innumerable studies have reported detection of HuNoVs in 3 to 20% of <5-year-old children hospitalized with diarrhea in developing countries. In order to probe the effects of malnutrition on norovirus (NoV) infections independent of host and environmental variability, we sought to study NoV infection in an animal model of malnutrition. Murine NoVs (MNVs) have become well-accepted surrogates for studying

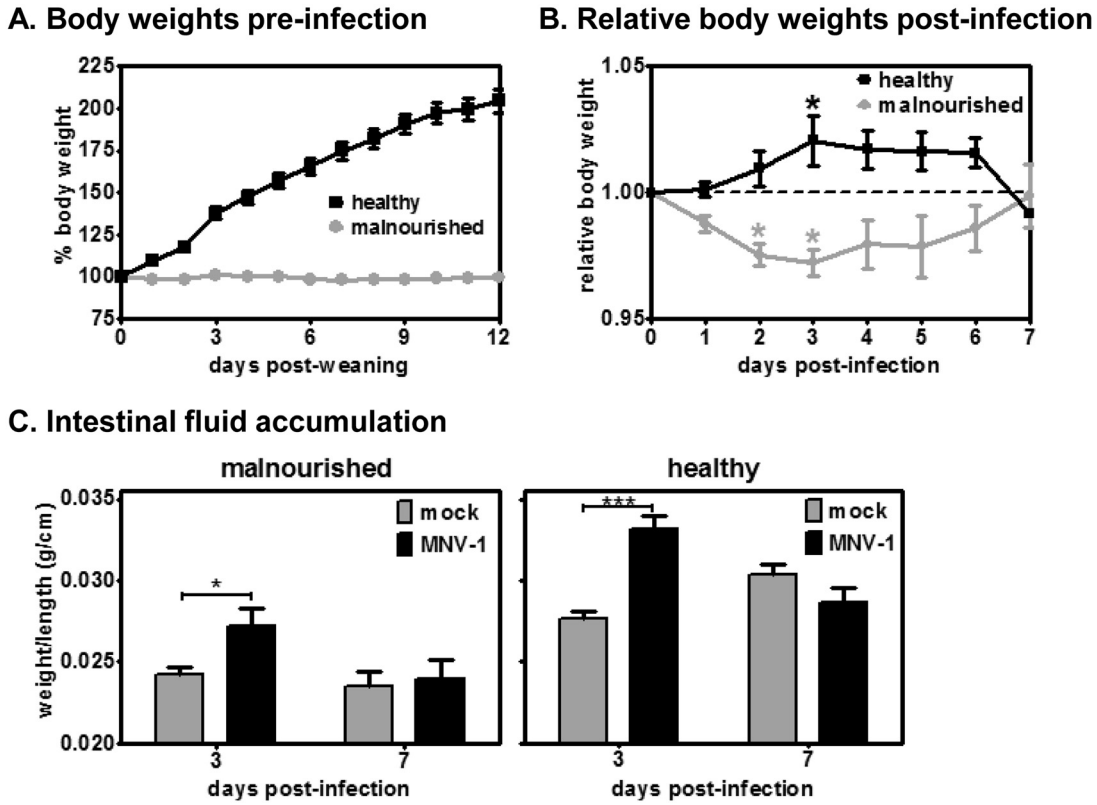

FIG 1 Both healthy and malnourished MNV-1-infected mice display intestinal fluid accumulation, but only malnourished mice lose weight. Groups of C57BL/6 mice were fed either a 2% (gray lines; malnourished) or 20% (black lines; healthy) protein diet for 12 days postweaning. (A) Each mouse ($n = 40$, total, in six experimental replicates) was weighed daily and compared to the day zero (d0) weight to calculate percent body weight over time. Data are presented as the average percent body weight per diet group. (B) Groups of mice on each diet ($n = 3$ to 5 per experiment in five experimental replicates) were mock inoculated or infected with 10^7 $TCID_{50}$ units MNV-1 p.o. and weighed daily for 7 dpi. The ratio of the average weight relative to that at 0 dpi in MNV-1-infected mice versus the average weight relative to that at 0 dpi in mock-inoculated mice for each diet group was calculated; the averages from all experiments were then averaged. The relative weights for mock-inoculated control mice were compared to those for MNV-1-infected mice in each diet group for statistical purposes. (C) Groups of C57BL/6 mice fed either a 2% or 20% protein diet were mock inoculated (gray bars) or infected with 10^7 $TCID_{50}$ units MNV-1 (black bars) p.o. At 3 and 7 dpi, groups of mice ($n = 5$ to 9, total, in three experimental replicates) were harvested, and the weight and length of the small intestine were recorded. Data are presented as the averaged weight per length for all mice per group. Groups of mice receiving mock inoculum versus MNV-1 infection in the same diet group at the same time point were compared for statistical purposes.

HuNoV pathogenesis since their initial discovery in 2003 (6–8). One commonly used murine model of malnutrition involves feeding mice a diet low in protein (9–15). Here we report that this specific form of malnutrition results in MNV-induced weight loss, impaired control of infection, muted antibody responses that correlate with an absence of protective immunity, enhanced viral evolution, and significant changes in the intestinal microbiota. Overall, we present a powerful new model system to probe the complex dynamic between nutrition, mucosal immunity, microbial composition, and the outcome of enteric viral infections.

RESULTS

Malnutrition is associated with norovirus-induced weight loss. To determine whether malnourished mice experience more severe MNV infection, groups of mice were weaned on either a 2% (malnourished group) or 20% (healthy group) protein-based diet. Healthy mice gained weight throughout this period, whereas malnourished mice failed to thrive (Fig. 1A), as expected. At 12 days postweaning, mice were administered mock inoculum or 10^7 50% tissue culture infective dose ($TCID_{50}$) units MNV-1 orally (p.o.) and weighed daily through 7 days postinfection (dpi). The weights of mock-inoculated and MNV-1-infected healthy mice were comparable at all time points except at 3 dpi, when the MNV-1-infected mice actually weighed slightly more than controls; in contrast, the weights of MNV-1-infected malnourished mice were reduced 3% compared to those of their mock-infected counterparts at 2 and 3 dpi (Fig. 1B). To investigate more thoroughly the pathogenic outcome of MNV-1 infection in healthy and malnourished mice, groups of mice were harvested at 1, 3, and 7 dpi and assessed for intestinal fluid accumulation as an indicator of gastroenteritis. We did not utilize visual scoring of fecal consistency as a measure of disease (as we have in previous studies [16–18]) because the feces in malnourished naive and MNV-1-infected mice are very hard and brittle. To our surprise, healthy mice infected with MNV-1 for 3 days presented with significant intestinal fluid accumulation (Fig. 1C); this pathology resolved by 7 dpi. No disease was observed in healthy infected mice at 1 dpi (data not shown). Malnourished mice also presented with significant intestinal fluid accumulation at 3 dpi (Fig. 1C). Groups of animals maintained on their respective diets for 5 weeks prior to infection displayed comparable phenotypes in terms of weight loss and intestinal fluid accumulation (data not shown). We conclude that

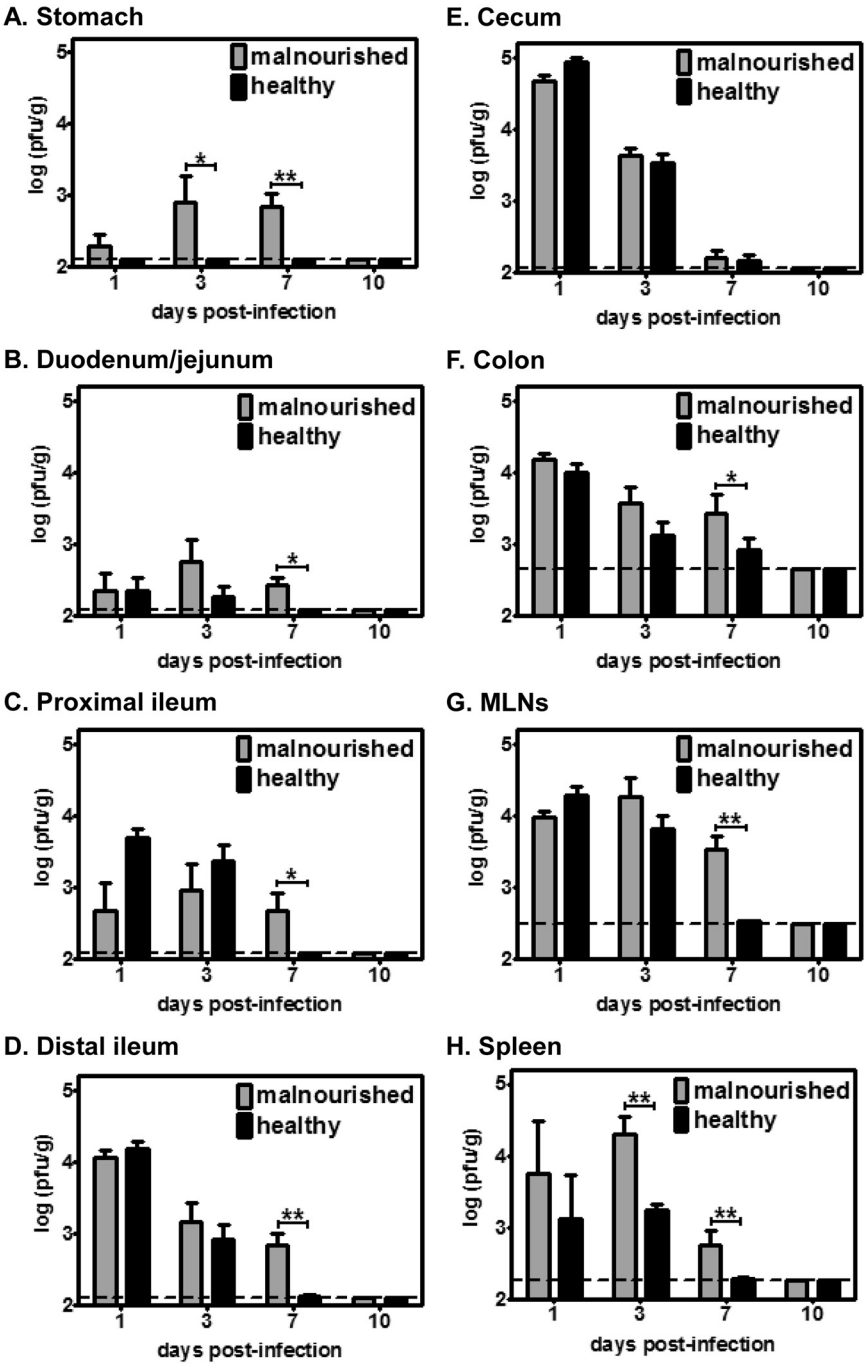

FIG 2 Control of MNV-1 infection is impaired in the malnourished host, and viral clearance is delayed. Groups of C57BL/6 mice were fed either a 2% (gray bars; malnourished) or 20% (black bars; healthy) protein diet for 12 days postweaning. Both groups were then infected with 10^6 $TCID_{50}$ units MNV-1 p.o. At 1 dpi ($n = 3$), 3 dpi ($n = 8$), and 7 dpi ($n = 7$), mice from each group were harvested, the indicated tissues were dissected, and viral titers were determined by plaque assay. The data are reported as PFU/g of tissue, and the data for all mice per group are averaged. The two diet groups were compared at each time point for each tissue for statistical purposes.

both healthy and malnourished mice are susceptible to symptomatic MNV-1 infection, but the overall outcome of infection is more severe in the malnourished host, as indicated by modest weight loss.

Malnutrition results in impaired control and delayed clearance of norovirus infection. We next tested whether malnutrition affects the magnitude and kinetics of *in vivo* virus replication by measuring virus loads at 1, 3, 7, and 10 dpi. While no virus was detectable in the stomachs of healthy mice, low levels were detected in the stomachs of malnourished mice 1 to 7 dpi (Fig. 2A). In the small intestine (duodenum/jejunum, proximal ileum, and distal ileum), colon, and mesenteric lymph nodes (MLNs), virus loads were comparable between the two groups at 1 and 3 dpi but were significantly higher in the malnourished mice at 7 dpi (Fig. 2B to D and 2F and G). In contrast, virus loads in the cecum were comparable between the two groups at all time points (Fig. 2E). Finally, splenic titers of virus were significantly higher in malnourished mice at 3 and 7 dpi (Fig. 2H). While virus was cleared from nearly all tissues of healthy mice by 7 dpi, clearance was delayed in malnourished mice, although it did occur by 10 dpi. It should be noted that in spite of the apparent viral clearance in both groups of mice by 7 to 10 dpi when measuring infectious virus, we were able to detect viral genomes in fecal samples of all mice as late as 50 dpi; this is relevant to viral diversity studies described below. Overall, malnutrition results in enhanced viral replication in the stomach and spleen and delayed clearance of infection in all tissues except the cecum.

Antiviral antibody responses are reduced in the malnourished host, correlating with ablated protective immunity. Because malnutrition has negative consequences on immune responses (9, 19–24), we next questioned whether mice fed a 2% protein diet would mount less effective MNV-specific immune responses. Groups of mice fed either a 2% or 20% protein diet were either mock inoculated or infected with 10^6 $TCID_{50}$ units MNV-1. Fecal pellets and serum were collected from each mouse at weekly intervals and tested in virus-specific enzyme-linked immunosorbent assay (ELISA) for IgA and IgG, respectively. There was a dramatic reduction in antiviral mucosal IgA at 1 to 6 weeks postinfection in malnourished mice compared to levels in their healthy counterparts (Fig. 3A). Surprisingly, then, the antiviral serum IgG responses were comparable between the two groups, with only slightly lower levels in malnourished mice at 1 and 6 weeks postinfection (Fig. 3B). Based on the reduced levels of antiviral mucosal antibody in MNV-1-immunized malnourished mice compared to those in healthy mice, we tested whether malnutrition impairs protective immunity to MNV-1, using viral tis-

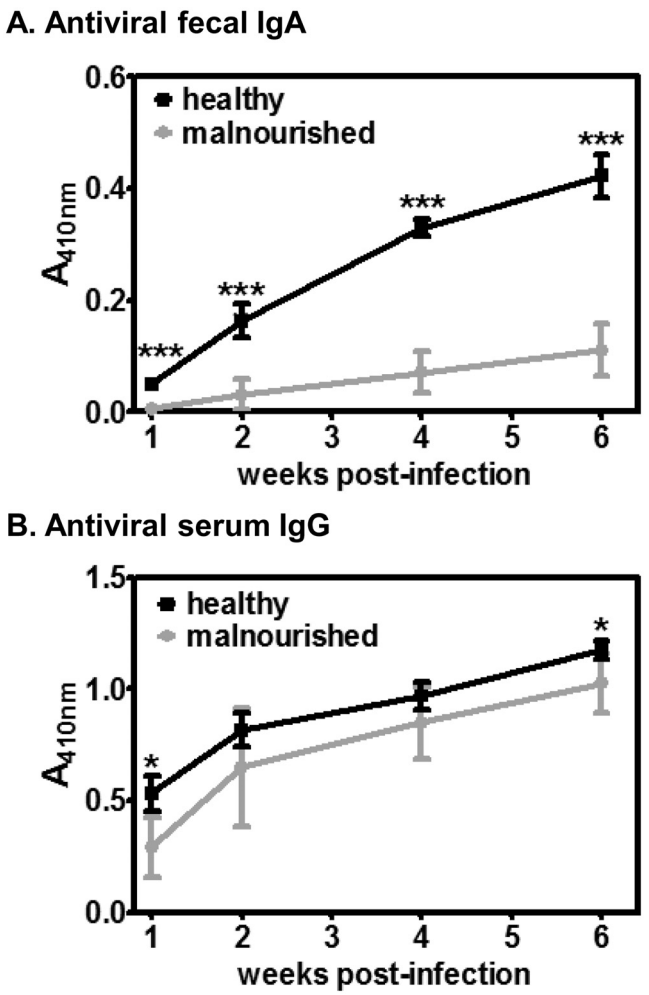

FIG 3 The antiviral antibody response is muted in malnourished hosts. Groups of C57BL/6 mice ($n = 8$ to 9, total, in two experimental replicates) were fed either a 2% (gray lines; malnourished) or 20% (black lines; healthy) protein diet for 12 days postweaning and then mock inoculated or infected with 10^6 $TCID_{50}$ units MNV-1 p.o. At 1, 2, 4, and 6 weeks postinfection, fecal pellets and serum were collected from each mouse. Virus-specific antibody was detected by standard ELISA using an anti-mouse IgA secondary for fecal lysates (A) or anti-mouse IgG secondary for serum samples (B). Data are reported as the average absorbance readings for all mice per condition. All samples collected from mock-inoculated mice tested negative (data not shown). The two diet groups were compared at each time point for statistical purposes.

sue titers as a measure of protection. We have previously reported that MNV-1 fails to elicit robust protective immunity in C57BL/6 mice (18, 25). It should be noted that previous studies used an intermediate immunization dose of 10^4 $TCID_{50}$ units MNV-1. We report here that the higher immunization dose of 10^6 $TCID_{50}$ units elicited measurable protective immunity in healthy C57BL/6 mice; in contrast, in malnourished mice, it failed to elicit comparable protective immune responses under these conditions (Fig. 4): while healthy mice displayed nearly undetectable secondary virus titers in all tissues analyzed, the secondary viral titers in malnourished mice were not reduced compared to primary titers in any tissue other than the spleen. Remarkably, immunized malnourished mice actually contained 10-fold-higher distal ileum and MLN virus loads than malnourished mice receiving primary infection. Because we observed quantifiable intestinal fluid accumulation in both healthy and malnourished mice at 3 dpi (see Fig. 1C), it was also possible to assess whether a prior virus challenge protected mice from disease. Indeed, healthy mice receiving a secondary MNV-1 challenge failed to display significant intestinal fluid accumulation (Fig. 5B). In contrast, intestinal fluid accumulation was statistically similar in malnourished mice receiving primary and secondary MNV-1 infections, and both groups displayed significantly increased levels of intestinal fluid compared to results for naive mice (Fig. 5A). Overall, malnourished mice are specifically impaired in their ability to mount a mucosal antibody response to MNV-1, correlating to an absence of protective immunity.

There is increased viral divergence in malnourished mice. Because host immune responses are known to be a strong driver of pathogen evolution and we observed significantly reduced MNV-specific immune responses in malnourished mice compared to those in healthy mice, we questioned whether the degree of NoV diversity would be influenced by nutritional status. Specifically, we measured genetic diversity in the MNV-1 open reading frame 2 (ORF2) gene over time in the feces of malnourished and healthy mice. We chose to investigate ORF2 diversity because it encodes the major structural protein of NoVs, referred to as VP1, which is subdivided into a conserved shell (S) domain and a more variable protruding (P) domain; the P domain can be further divided into the P1 stalk region and the hypervariable P2 region making up the tips of the arches (26). Evidence indicates that antigenic and receptor binding domains are located in P2 (see reference 27 and references therein). Moreover, VP1 plays a role in dictating MNV virulence (28, 29). Diversity was modestly lower in both groups of animals than the average diversity in the infecting viral stock at 35 and 50 dpi, suggesting a possible population bottleneck during the *in vivo* evolution of the virus (data not shown). Average divergence from the infecting viral stock was also not significantly different between healthy and malnourished hosts at 35 dpi (data not shown). However, it was significantly higher in malnourished mice than in controls at 50 dpi (Fig. 6). Importantly, the number of nonsynonymous (dN) substitutions compared to the sequence of the infecting viral swarm was also significantly higher in malnourished animals than in healthy controls at this time point, while synonymous (dS) substitutions were not significantly different (Fig. 6). Since an increase in dN generally indicates an increased fixation rate of coding changes that may be due to the emergence of variants with higher fitness, we investigated the location of coding changes in the VP1 P domain. Specifically, we mapped each mutation detected in the two diet groups at 35 and 50 dpi on the MNV-1 VP1 P-domain crystal structure. There were more coding changes observed in the VP1 P domain of malnourished mice at 50 dpi than at 35 dpi (Fig. 7), consistent with immune-driven evolution. Moreover, there were more changes in the VP1 P domain for malnourished mice at 50 dpi than for healthy mice at the same time point (Fig. 7), revealing that MNV-1 evolves more readily in a malnourished environment.

Malnutrition and norovirus infection are associated with dramatic changes in the composition of the microbiota. The intestinal microbiota is modified by nutrition (30–33) and itself shapes mucosal immunity (34–36). Moreover, the microbiota can directly regulate viral infections (37, 38), and enteric viral infections can cause alterations in the microbial composition (39, 40), underscoring the complex and interdependent relationships be-

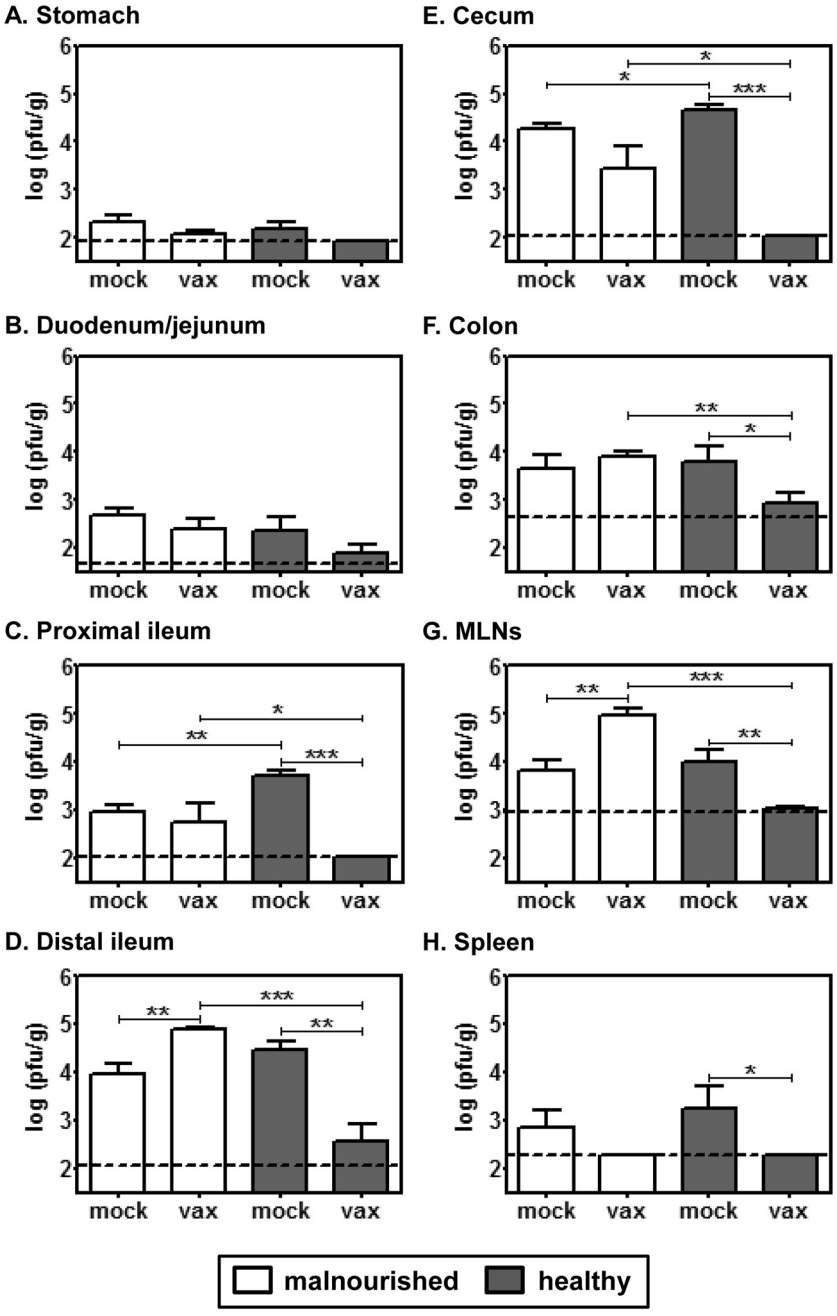

FIG 4 MNV-1 protective immunity is ablated by malnutrition as assessed by titers of virus in tissue. Groups of mice ($n = 5$) fed a 2% (white bars; malnourished) or 20% (gray bars; healthy) protein diet were either mock inoculated (labeled "mock" on *x* axis) or immunized with 10^6 $TCID_{50}$ units MNV-1 (labeled "vax" on *x* axis for vaccinated). Six weeks later, all mice were challenged with 10^7 $TCID_{50}$ units MNV-1 p.o. At 1 day post-secondary challenge, mice were sacrificed and the indicated tissues were harvested for virus load determination using a standard plaque assay. The data for all mice per condition were averaged, and the limits of detection are indicated by dashed lines. Groups compared for statistical analysis include diet-matched mock versus vax, mock on 2% versus 20% protein diets, and vax on 2% versus 20% protein diets.

tween nutritional status, mucosal immunity, and the microbiota that drive host responses to enteric infections. To test whether malnutrition in our system alters the microbiota, groups of mice fed either a 2% or 20% protein diet were administered mock inoculum or 10^7 $TCID_{50}$ units MNV-1. Fecal samples from individual mice at 0 to 5 dpi were analyzed for microbial composition using 454 pyrosequencing of the bacterial 16S rRNA gene. When samples collected from the two diet groups at 0 dpi were compared, there was a significant reduction in the proportion of *Bacteroidetes* and a concurrent increase in *Firmicutes* for malnourished mice compared to results for their healthy counterparts at the phylum level (Fig. 8A). In healthy mice, MNV-1 infection also altered the microbiome, with a significant decrease in the *Bacteroidetes*/*Firmicutes* ratio compared to that for mock-inoculated

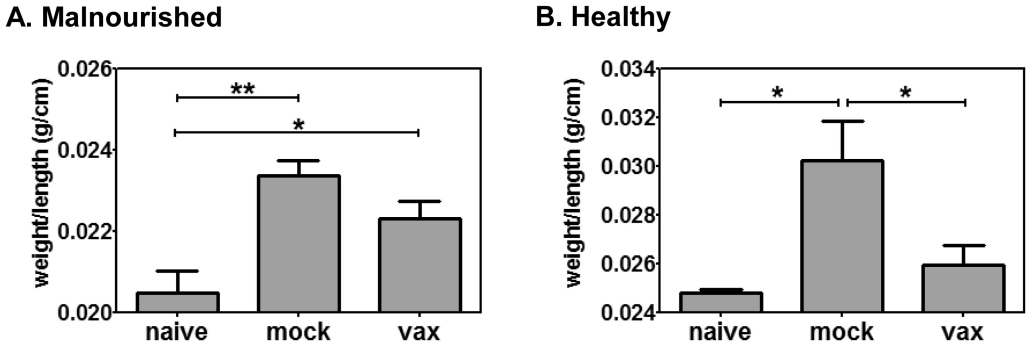

FIG 5 MNV-1 protective immunity is ablated by malnutrition as assessed by intestinal fluid accumulation. Groups of mice fed a 2% (A) or 20% (B) protein diet were either mock inoculated (labeled "mock" on *x* axis; $n = 4$) or immunized with 10^6 $TCID_{50}$ units MNV-1 (labeled "vax" on *x* axis, for vaccinated; $n = 6$). Six weeks later, all mice were challenged with 10^7 $TCID_{50}$ units MNV-1 p.o. A third group of mice was included for each diet that received mock inoculum at both infections (labeled "naïve" on *x* axis; $n = 3$). At 3 days post-secondary challenge, mice were sacrificed and intestinal fluid was measured as described in Materials and Methods. The data for all mice per condition were averaged. Groups compared for statistical analyses include diet-matched naive versus mock, naive versus vax, and mock versus vax.

controls; no changes were observed in malnourished mice as a result of MNV-1 infection at the phylum level (Fig. 8B). Data are presented for 5 dpi; a similar pattern was observed at all time points postinfection (data not shown). By categorizing our microbiome data sets into operational taxonomic units (OTUs), we identified three OTUs that displayed highly significant and inverse *z* scores when comparing the two diet groups. The closest match of the representative sequence in these OTUs to database entries was to Gram-negative bacterium cL10-2b-4, *Clostridiales* bacterium r41, and human intestinal firmicute CJ31. These bacterial species are thus likely regulated by nutritional status. We also identified one OTU—matching closest to rumen_bacterium_RC-2—that was affected in its abundance upon MNV-1 infection in both diet groups, suggesting a specific correlation with viral infection.

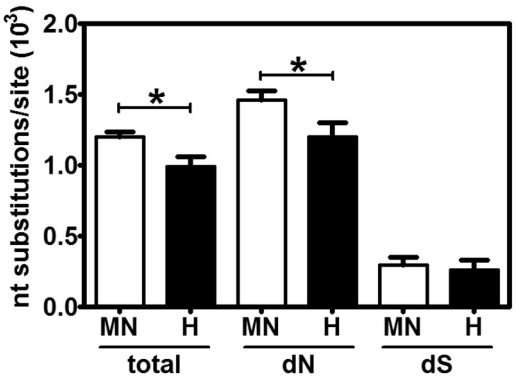

FIG 6 MNV-1 genetic distance from the infecting viral stock over time. Groups of mice ($n = 5$) fed either a 2% (white bars; "MN" on the *x* axis, for malnourished) or 20% (black bars; "H" on the *x* axis, for healthy) protein diet were infected with 10^6 $TCID_{50}$ units MNV-1. At 50 dpi, fecal pellets were collected and processed as described in Materials and Methods. The virus stock used for inoculation was analyzed in the same manner. This sequence set was used to estimate average genetic divergence, i.e., pairwise distances between sequences at a given time point and the infecting viral stock (*y* axis) for each animal-specific data set (*x* axis). Here we report maximum-likelihood estimated divergence in all nucleotide ("total" on *x* axis), nonsynonymous ("dN" on *x* axis), and synonymous ("dS" on *x* axis) substitutions per site estimated using the Nei-Gojobori method. Statistical analysis to compare the two diet groups was performed with the Mann-Whitney *U* test. Statistically significant *P* values (<0.05) are shown.

DISCUSSION

Malnourished mice develop more severe and prolonged MNV-1 infections. In general, malnourished hosts are highly susceptible to severe and prolonged viral infections (3). Circumstantial evidence indicates that HuNoV infections are more severe in the context of malnutrition—HuNoV infections are responsible for 3 to 20% of pediatric diarrheal cases that require hospitalization in developing countries (41–52), whereas HuNoV-infected children in industrialized nations develop self-limited gastroenteritis that rarely requires treatment. Data from our new model of MNV infection in malnourished mice provide unequivocal evidence of nutrition-regulated NoV susceptibility: malnourished mice developed more severe MNV-1 infections as evidenced by weight loss (Fig. 1B) and impaired control of viral replication in the stomach and spleen (Fig. 2). It should be noted that both healthy and malnourished mice were symptomatically infected with MNV-1, as indicated by increased fluid within the intestinal lumen at 3 dpi (Fig. 1C). We have previously published that MNV-1 does not induce intestinal fluid accumulation in healthy wild-type mice (16). Since previous studies were carried out at Louisiana State University Health Sciences Center, Shreveport, while current studies were performed at University of Florida, Gainesville, it is possible that institutional variability in intestinal microbial composition or other environmental factors account for our discrepant results. We excluded diet as the confounding variable since mice fed either the 20% protein diet used in the current study (Harlan TD.91352) or the diet used in previous studies (Harlan Teklad LM-485) displayed comparable intestinal fluid accumulation at 3 dpi (data not shown). In spite of the observed institutional variability, this quantitative measure of intestinal fluid accumulation provides further support that MNV infection indeed replicates HuNoV pathogenesis in causing gastroenteritis in immunocompetent hosts. Although malnourished mice did not develop more severe gastroenteritis as measured by intestinal fluid accumulation, they did lose weight upon MNV-1 infection, while healthy mice maintained normal body weight. Thus, although both groups developed symptomatic infection, the outcome was more severe in the malnourished host.

Malnourished mice were also delayed in clearing MNV-1 from a wide range of tissues: while healthy mice cleared virus from

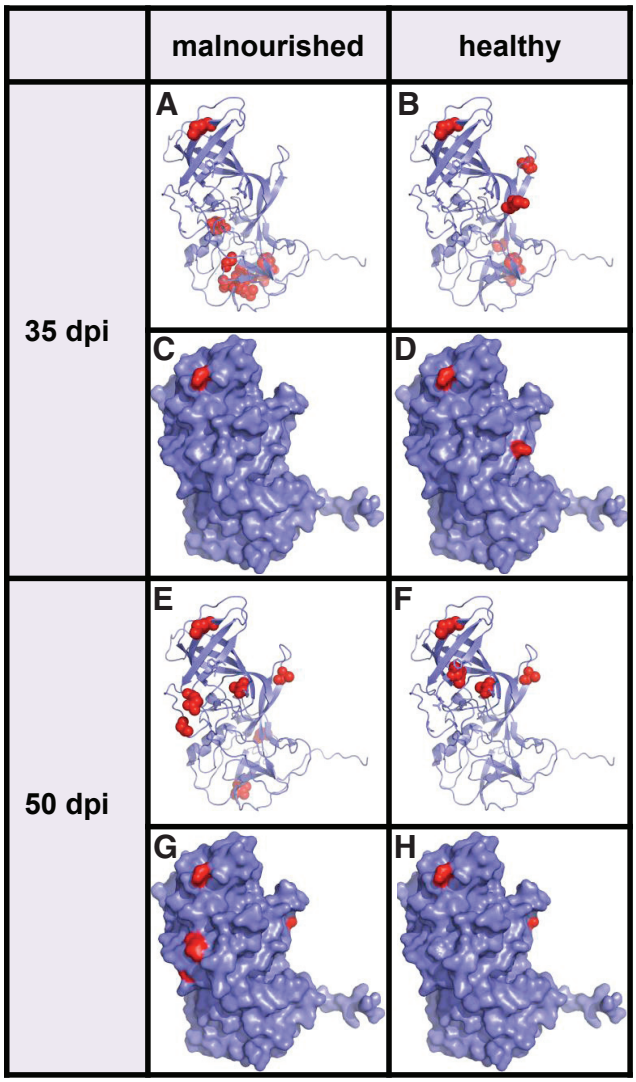

FIG 7 Mapping of mutations on the MNV-1 VP1 P-domain crystal structure. The crystal structure of the P domain of MNV-1 VP1 (amino acids [aa] 225 to 541; PDB 3LQE) is shown. In all panels, the protein is shown in blue, and the nonsynonymous mutations observed in our study are shown as red spheres. The protein backbone depicted in ribbon diagrams (A, B, E, and F) and the molecular surface (C, D, G, and H) are represented for both diet groups at 35 and 50 dpi. While a majority of the mutations observed in both diet groups at 35 dpi appeared to be solvent inaccessible and segregated in the P1 domain of VP1, a majority of the mutations observed at 50 dpi largely clustered on the solvent-exposed surface of the P2 domain. A significantly higher number of such mutations were detected in the 2% protein diet group at both time points.

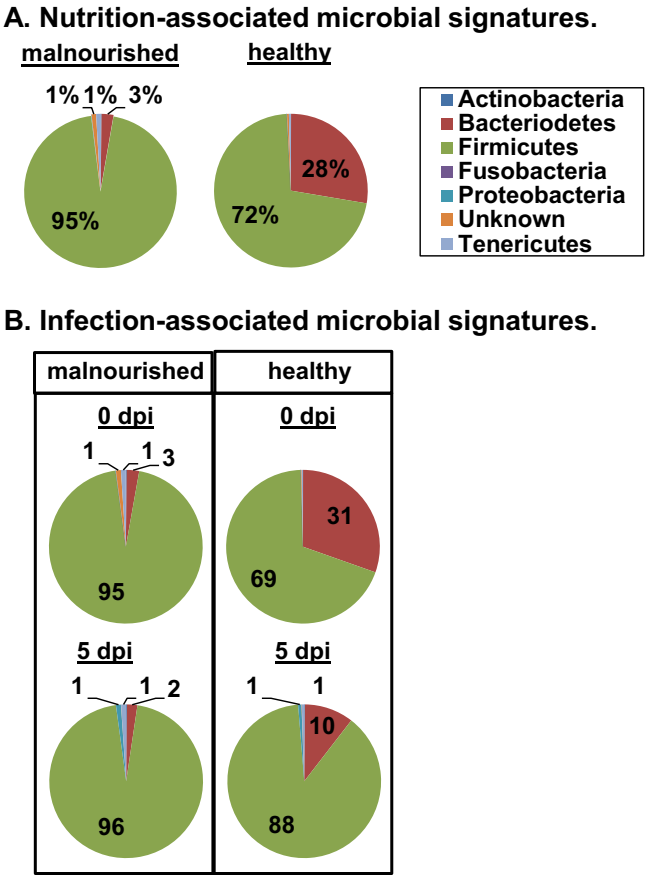

FIG 8 The composition of the microbiota is altered by protein malnutrition and MNV-1 infection. Groups of mice ($n = 8$) were fed either a 2% (malnourished) or 20% (healthy) protein diet. Three mice per diet were mock inoculated, while the other five mice were infected with 10^7 $TCID_{50}$ units MNV-1. Fecal samples were collected from individual mice at 0, 1, 2, 3, 4, and 5 dpi, and the microbiome composition was determined by 454 sequencing of the hypervariable V1-to-V3 region of the bacterial 16S rRNA gene. (A) The microbiome distribution of each diet group at 0 dpi at the phylum level is presented. (B) Phylum data for the infected mice at 0 and 5 dpi are shown for each diet group.

nearly all tissues by 7 dpi (with the exception of very low levels of virus remaining in the cecum and colon), malnourished mice failed to clear virus from the stomach, all regions of the small and large intestines, MLNs, and spleens until 10 dpi (Fig. 2). It should be noted that reverse transcription-PCR (RT-PCR) amplification of the viral genome is much more sensitive than determining titers of infectious virus by plaque assay. Underscoring this point, we amplified viral the genome from fecal samples of infected mice at 50 dpi irrespective of diet (Fig. 6). Thus, although infectious virus was undetectable by 7 to 10 dpi in both diet groups, the mice remained persistently infected at a low level for at least 50 dpi. It has been reported that MNV-1 establishes only acute infections that are cleared by 7 dpi in healthy wild-type mice even when using a sensitive quantitative RT-PCR (qRT-PCR)-based detection approach (53); however, it is becoming increasingly clear within the NoV community that viral persistence is influenced by yet-to-be-identified environmental factors. Our data clearly show that MNV-1 established persistent infections in wild-type C57BL/6 mice in the environment under which our mice are housed, albeit at a very low level. Importantly, this allowed us to study intrahost viral evolution in wild-type mice (see below). Collectively, MNV-1 caused more severe and prolonged infections in malnourished mice than in healthy mice.

Malnourished mice are impaired in their ability to induce protective immunity to MNV-1. Malnutrition generally results not only in a reduced ability to control mucosal infections but also in a reduced ability to develop protective immunity toward subsequent reinfections, underscored by the poor response to certain oral vaccines in malnourished individuals (54, 55). This is also reflected in our new model system: malnourished mice mounted a dramatically reduced mucosal IgA and slightly reduced serum IgG

response to MNV-1 compared to those of healthy hosts (Fig. 3). Elucidating the immunological basis for this impaired humoral immune response could have broad applicability considering that malnourished hosts also develop reduced antibody responses to influenza virus, *Streptococcus pneumoniae*, *Plasmodium falciparum*, the measles virus vaccine, and a DNA vaccine against tuberculosis (56–59). Importantly, reduced MNV-1-specific antibody levels in immunized malnourished mice correlated with a loss of protection from a secondary challenge when viral tissue titers (Fig. 4) and intestinal fluid accumulation (Fig. 5) were used as indicators of protection. In fact, virus titers for rechallenged malnourished mice were even higher than primary titers in certain tissues. One explanation for increased virus loads in rechallenged malnourished mice is that malnourished hosts become persistently infected and thus contain residual primary virus titers. However, we did not detect infectious virus at 10 dpi in a large panel of tissues (Fig. 2), so this possibility seems unlikely. Another possibility that we are currently exploring is immune-mediated enhancement of infection. For example, the reduced antibody response in malnourished mice may be below a concentration threshold, or of insufficient affinity or avidity, to neutralize virus and instead enhance interaction with Fc receptors on permissive phagocytic cells, as observed for Dengue virus (60). Dissecting the basis of this immunization-enhanced infection has significant implications regarding HuNoV vaccination strategies in the developing world. Overall, there were no significant reductions in secondary virus titers compared to primary titers in malnourished mice except in the spleen, suggesting that malnutrition specifically reduces the induction or maintenance of a mucosal immune response. This idea is further supported by the dramatic reduction in mucosal but not peripheral antiviral antibody levels. Finally, the data presented in Fig. 5 represent the first protection study performed in the MNV model system using disease in a wild-type host as a readout. The availability of a quantifiable measure of disease should prove valuable in testing immunization and therapeutic strategies for NoV infections.

There is greater MNV-1 diversity in malnourished mice than in healthy mice. Grenfell et al. presented a viral phylodynamic framework that predicts that an RNA virus will adapt most readily under conditions of intermediate immunity in which the virus can replicate efficiently in the face of a weak immune response (61). Based on the reduced antiviral antibody responses and delayed MNV-1 clearance in our malnourished hosts, we thus questioned whether they would support a higher level of NoV evolution than healthy hosts. Indeed, MNV-1 adapted more readily in malnourished mice than in healthy mice by 50 dpi, with a specific increase in VP1 P-domain coding changes (Fig. 6 and 7). Interestingly, there was also a trend toward lower diversity in the viral swarms of both groups of mice than in the original inoculum by 35 dpi, suggesting that in both models the evolution of the virus may be characterized by a population bottleneck. When considered together, these collective results suggest that increased viral replication in malnourished hosts early in infection (e.g., see Fig. 2) establishes a complex viral quasispecies that more readily evolves in response to immune pressure. They also suggest that the most likely HuNoV reservoirs are individuals with suboptimal but not ablated immune responses, including malnourished hosts. Consistent with this, Siebenga et al. observed for HuNoV-infected people that the number of amino acid changes over time was higher in patients with intermediate immunocompromise than in more severely immunocompromised patients (62).

Although a majority of adaptive mutations were detected in only one diet group, a lysine-to-glutamate change at VP1 position 296 became predominant in both diet groups over time. Specifically, 7% of virus inoculum clones contained a glutamate residue at this position, while 59% and 75% of clones obtained from fecal pellets of our collective group of mice contained a glutamate at 35 and 50 dpi, respectively. This specific change arises during cell culture passaging of MNV-1 (29, 63) and has been associated with attenuation in STAT1$^{-/-}$ mice (28, 29). Most MNV strains other than MNV-1 identified to date have a glutamate at this position (29), suggesting a fitness advantage to the virus since it is routinely selected for *in vitro* and *in vivo* in spite of its attenuating phenotype in interferon-deficient mice. Amino acid 296 occurs in the hypervariable P2 region of VP1, so a lysine-to-glutamate change may alter the efficiency of receptor engagement.

Malnutrition and MNV-1 infection independently influence the composition of the microbiota. Our data provide strong evidence that both malnutrition and NoV infection can heavily influence the gut microbial composition, in particular the *Bacteroidetes*/*Firmicutes* ratio. A similar decreased *Bacteroidetes*/*Firmicutes* ratio has been observed in malnourished Bangladeshi children relative to their adequately nourished counterparts (64), in obese mice (65), in obese people (66), in mice with a humanized microbiota that are switched from a low-fat, plant polysaccharide-rich diet to a high-fat, plant polysaccharide-low Western diet (33), in European children relative to children in Burkina Faso (30), and in antibiotic-treated mice (67). A *Bacteroides*-enriched enterotype is highly associated with animal protein, with enterotype members deriving their energy primarily from proteins and carbohydrates (32, 68), providing a functional clue as to the reduced proportion of *Bacteroides* species in a protein-deficient environment. It is intriguing that MNV-1 infection of healthy mice caused a shift to a "malnourished" microbial signature. Early studies of HuNoV infections in human volunteers demonstrated a transient decrease in activity of specific brush border enzymes involved in digestion and nutrient absorption (69), so it is possible that this causes an acute state similar to malnutrition that alters the microbial community within the intestine. Nelson et al. observed a similarly decreased proportion of *Bacteroidetes* in ca. 20% of a small study group of HuNoV-infected individuals in the United States, although these individuals had an increased proportion of *Proteobacteria*, in contrast to the increased proportion of *Firmicutes* observed in MNV-1-infected healthy mice (40). Future studies will aim to investigate the specific impact of these microbial changes on the outcome of NoV infection and viral evolution. These changes could be direct (e.g., recent work shows an increase in free sialic acid in the gut lumens of antibiotic-treated mice displaying a dramatically decreased *Bacteroides*/*Firmicutes* ratio [67]; multiple MNV strains utilize sialic acid as an attachment receptor, so luminal sialic acid could in effect neutralize virus) or indirect (e.g., *Bacteroides* species can induce specific types of immune responses [70–73], so their absence may influence the host antiviral response).

Overall, we present an extensive characterization of MNV infection in malnourished hosts, setting the foundation to probe the complex relationships between nutritional status, mucosal immunity, and the microbiota that shape the overall host response to enteric pathogens.

MATERIALS AND METHODS

Mice and diets. Pregnant wild-type C57BL/6 mice were purchased from Charles River Laboratories (Wilmington, MA) and housed in animal facilities at the University of Florida under specific-pathogen-free conditions. For all experiments, sex-matched 3-week-old C57BL/6 mice were randomly assigned at the time of weaning to isocaloric diets (Harlan Laboratory, Maine) containing 2% (TD.92203) or 20% (TD.91352) protein; the diets were made isocaloric by substituting sugar and starch for the protein. Mice were maintained on their respective diets throughout the experiments. All animal research conducted in the present study was approved by the Institutional Animal Care and Use Committee at the University of Florida (study number 201107166 or 201107538).

Virus and infections. MNV-1 isolate CW3 (16) at passage 7 (referred to herein as MNV-1) was used in all experiments. A virus stock was generated by centrifuging infected RAW 264.7 cell lysates through a sucrose cushion and fractionating on a cesium chloride gradient, as previously described (16, 63), and titrated using a standard $TCID_{50}$ assay (53). A mock inoculum stock was prepared in parallel using RAW 264.7 cell lysate from uninfected cultures. For all experiments, mice were inoculated perorally (p.o.) with 25 μl MNV-1 or mock inoculum. When virus loads were determined, mice were perfused and tissues were dissected, weighed, and homogenized in medium by bead beating using 1.0-mm zirconia/silica beads (BioSpec Products, Inc.). Plaque assays of tissue samples were performed as previously described (17, 63), and data are presented as PFU per gram of tissue.

Gastroenteritis assay. Intestinal fluid accumulation was assessed using a standard assay (16, 17). In brief, the small intestine was ligated at pyloric and cecal junctions, dissected, weighed, and measured for length. Intestinal fluid accumulation was indicated by a weight/length ratio that was increased for infected mice over that for controls.

Virus-specific ELISA. Submandibular puncture was used to collect serum from mice at the indicated time points postinfection. Fecal pellets (0.05 g) were collected into 0.5-ml phosphate-buffered saline (PBS) containing protease inhibitor cocktail (Sigma), homogenized, and centrifuged at 20,000 $\times$ *g* at 4°C for 20 min. An MNV-1-specific ELISA has been previously described (25). In brief, 96-well plates were coated with 250 ng of MNV-1 recombinant VP1/VP2 (rVP1/2) protein and incubated at 4°C overnight. Serum samples diluted 1:20 or fecal lysates diluted 1:10 were applied, followed by anti-mouse IgG or anti-mouse IgA conjugated to horseradish peroxidase (HRP) as a secondary antibody, respectively. After addition of the ABTS [2,2'-azinobis(3-ethylbenzthiazolinesulfonic acid] substrate, absorbance values were read at 410 nm using a Spectramax M2 plate reader. A standard curve was generated for each plate using serial dilutions of a positive-control MNV-1 serum sample to ensure plate-to-plate consistency. Serum and fecal samples from an equivalent number of mock-inoculated control mice were tested in parallel with experimental samples. The average value of controls was used as an indication of baseline detection levels.

Viral diversity. Fecal pellets from mice administered mock inoculum or 10^7 $TCID_{50}$ units MNV-1 p.o. were collected into 1 ml RNALater (Qiagen) at the indicated time points and flash-frozen in a dry ice-ethanol bath. The fecal samples were homogenized by mashing with a pipette tip and vortexing. Samples were clarified by centrifugation, passed through a 0.45-μM filter, and RNA extracted using the QIAamp viral RNA minikit (Qiagen). The RNA was converted to cDNA using the ImProm-II reverse transcription system (Promega), and ORF2-specific primers (ATGAGGA TGAGTGATGGCGCAGC; TTATTGTTTGAGCATTCGGCCTG) were used with PfuUltra II Fusion HotStart DNA polymerase (Agilent Technologies) to amplify the full-length 1,626-nucleotide (nt) ORF2 gene. After cloning the PCR products into pCR-Blunt II-TOPO (Life Technologies), 10 to 15 clones per individual were sequenced using universal T7 and SP6 primers and two virus-specific primers: MNV1.F8 (TGTTGCCC TTGTACCACCCTATTT) and MNV1.R9 (CACGAACCCTGCCATCC AC). The MNV-1 stock used for inoculation was sequenced and analyzed in the same manner. Multiple sequence alignments were generated with the BioEdit software program (http://www.mbio.ncsu.edu/bioedit/bioedit.html). A neighbor-joining phylogenetic tree, based on pairwise *p*-distances (nucleotide changes per site), was inferred for all sequences using the MEGA 5.0 software program (74) to detect hypermutated sequences, which were excluded from subsequent analyses. Average viral diversity (i.e., the average pairwise distance among sequences at the same time point) and divergence (i.e., average pairwise distance between sequences at a given time point and the infecting viral stock), in nucleotide substitutions per site, were estimated with the maximum-likelihood composite method implemented in MEGA 5.0. The numbers of synonymous substitutions per synonymous site (dS) and nonsynonymous substitutions per nonsynonymous site (dN) were also estimated using the Nei-Gojobori method in MEGA 5.0. Standard errors for each estimate were obtained by bootstrapping (500 replicates).

Microbiota analysis. Fecal samples were collected from two groups each of mock-inoculated ($n = 3$) and MNV-1-infected ($n = 5$) mice at 0, 1, 2, 3, 4, and 5 dpi; one group was fed a 2% protein diet, while the other was fed a 20% protein diet, as described above. For each fecal sample, DNA was extracted from 100 to 150 mg feces using a modified Qiagen stool DNA extraction protocol with a bead-beating step (75). The V1-to-V3 hypervariable region of the bacterial 16S rRNA gene was then amplified with a bar-coded pyrosequencing primer based on the universal primers 27F and RF33 and sequenced on a Roche 454 GS-FLX Plus system. From the resulting raw data set, low-quality sequences or sequences with a length less than 150 nt were removed. We used the ESPRIT-Tree algorithm, which maintains the binning accuracy of ESPRIT while improving computational efficiency of hierarchical clustering to bin sequences into operational taxonomic units (OTUs) using similarity levels from 99% (species/strain level) to 80% (phylum level) (76, 77). We used the QIIME software package to calculate Chao rarefaction diversity and UniFrac distances for comparing α and β diversity, respectively (78, 79). Using the Excel program and a heat map generator, we utilized proportion analysis to create summary pie charts and bar charts of individual data sets and heatmaps by OTU *z* score and prevalence.

Statistical analysis. All data analyses presented in Fig. 1 to 6 were performed using GraphPad Prism software. In all graphs, standard errors of means were used to define error bars and *P* values were determined using unpaired two-tailed *t* tests. One asterisk represents *P* values of 0.01 to 0.05, two asterisks represent *P* values of 0.001 to 0.01, and three asterisks represent *P* values of less than 0.001. A one-tailed Mann-Whitney U test was used to assess whether average viral divergence in the malnourished group was significantly higher ($P < 0.05$) than that in the healthy group at 35 dpi and 50 dpi.

ACKNOWLEDGMENT

This work was supported by Seed Fund 13-1, provided by the Emerging Pathogens Institute of the University of Florida.

REFERENCES

1. **Koo HL, Neill FH, Estes MK, Munoz FM, Cameron A, DuPont HL, Atmer RL.** 2013. Noroviruses: the most common pediatric viral enteric pathogen at a large university hospital after introduction of rotavirus vaccination. J. Pediatr. Infect. Dis. **2:**57–60. http://dx.doi.org/10.1093/jpids/pis070.
2. **Payne DC, Vinjé J, Szilagyi PG, Edwards KM, Staat MA, Weinberg GA, Hall CB, Chappell J, Bernstein DI, Curns AT, Wikswo M, Shirley SH, Hall AJ, Lopman B, Parashar UD.** 2013. Norovirus and medically attended gastroenteritis in U.S. children. N. Engl. J. Med. **368:**1121–1130. http://dx.doi.org/10.1056/NEJMsa1206589.
3. **Beck MA.** 1996. The role of nutrition in viral disease. J. Nutr. Biochem. **7:**683–690. http://dx.doi.org/10.1016/S0955-2863(96)00132-5.
4. **Beck MA, Handy J, Levander OA.** 2004. Host nutritional status: the neglected virulence factor. Trends Microbiol. **12:**417–423. http://dx.doi.org/10.1016/j.tim.2004.07.007.
5. **Patel MM, Widdowson MA, Glass RI, Akazawa K, Vinjé J, Parashar UD.** 2008. Systematic literature review of role of noroviruses in sporadic gastroenteritis. Emerg. Infect. Dis. **14:**1224–1231. http://dx.doi.org/10.3201/eid1408.071114.

6. **Wobus CE, Thackray LB, Virgin HW.** 2006. Murine norovirus: a model system to study norovirus biology and pathogenesis. J. Virol. **80:** 5104–5112. http://dx.doi.org/10.1128/JVI.02346-05.
7. **Karst SM.** 2010. Murine norovirus pathogenesis and immunity. Caliciviruses: molecular and cellular virology, p 183–203. Horizon Scientific Press, Poole, United Kingdom.
8. **Karst SM, Wobus CE, Lay M, Davidson J, Virgin HW.** 2003. STAT1-dependent innate immunity to a Norwalk-like virus. Science **299:** 1575–1578. http://dx.doi.org/10.1126/science.1077905.
9. **Iyer SS, Chatraw JH, Tan WG, Wherry EJ, Becker TC, Ahmed R, Kapasi ZF.** 2012. Protein energy malnutrition impairs homeostatic proliferation of memory CD8 T cells. J. Immunol. **188:**77–84. http://dx.doi.org/10.4049/jimmunol.1004027.
10. **Malafaia G, Serafim TD, Silva ME, Pedrosa ML, Rezende SA.** 2009. Protein-energy malnutrition decreases immune response to Leishmania chagasi vaccine in BALB/c mice. Parasite Immunol. **31:**41–49. http://dx.doi.org/10.1111/j.1365-3024.2008.01069.x.
11. **Marroquí L, Batista TM, Gonzalez A, Vieira E, Rafacho A, Colleta SJ, Taboga SR, Boschero AC, Nadal A, Carneiro EM, Quesada I.** 2012. Functional and structural adaptations in the pancreatic A-cell and changes in glucagon signaling during protein malnutrition. Endocrinology **153:**1663–1672. http://dx.doi.org/10.1210/en.2011-1623.
12. **Shimosato T, Tomida K, Otani H.** 2011. Effect of Lactobacillus pentosus ONRIC b0240 on intestinal IgA production in mice fed differing levels of protein. J. Agric. Food Chem. **59:**2646–2651. http://dx.doi.org/10.1021/jf104240d.
13. **Soriano S, Gonzalez A, Marroquí L, Tudurí E, Vieira E, Amaral AG, Batista TM, Rafacho A, Boschero AC, Nadal A, Carneiro EM, Quesada I.** 2010. Reduced insulin secretion in protein malnourished mice is associated with multiple changes in the B-cell stimulus-secretion coupling. Endocrinology **151:**3543–3554. http://dx.doi.org/10.1210/en.2010-0008.
14. **Steevels TA, Hillyer LM, Monk JM, Fisher ME, Woodward BD.** 2010. Effector/memory T cells of the weanling mouse exhibit type 2 cytokine polarization *in vitro* and *in vivo* in the advanced stages of acute energy deficit. J. Nutr. Biochem. **21:**504–511. http://dx.doi.org/10.1016/j.jnutbio.2009.02.007.
15. **Teo HK, Price P, Papadimitriou JM.** 1991. The effects of protein malnutrition on the pathogenesis of murine cytomegalovirus disease. Int. J. Exp. Pathol. **72:**67–82.
16. **Mumphrey SM, Changotra H, Moore TN, Heimann-Nichols ER, Wobus CE, Reilly MJ, Moghadamfalahi M, Shukla D, Karst SM.** 2007. Murine norovirus 1 infection is associated with histopathological changes in immunocompetent hosts, but clinical disease is prevented by STAT1-dependent interferon responses. J. Virol. **81:**3251–3263. http://dx.doi.org/10.1128/JVI.02096-06.
17. **Kahan SM, Liu G, Reinhard MK, Hsu CC, Livingston RS, Karst SM.** 2011. Comparative murine norovirus studies reveal a lack of correlation between intestinal virus titers and enteric pathology. Virology **421:** 202–210. http://dx.doi.org/10.1016/j.virol.2011.09.030.
18. **Liu G, Kahan SM, Jia Y, Karst SM.** 2009. Primary high-dose murine norovirus 1 infection fails to protect from secondary challenge with homologous virus. J. Virol. **83:**6963–6968. http://dx.doi.org/10.1128/JVI.00284-09.
19. **Chatraw JH, Wherry EJ, Ahmed R, Kapasi ZF.** 2008. Diminished primary CD8 T cell response to viral infection during protein energy malnutrition in mice is due to changes in microenvironment and low numbers of viral-specific CD8 T cell precursors. J. Nutr. **138:**806–812.
20. **Fox CJ, Hammerman PS, Thompson CB.** 2005. Fuel feeds function: energy metabolism and the T-cell response. Nat. Rev. Immunol. **5:**844–852. http://dx.doi.org/10.1038/nri1710.
21. **Ing R, Su Z, Scott ME, Koski KG.** 2000. Suppressed T helper 2 immunity and prolonged survival of a nematode parasite in protein-malnourished mice. Proc. Natl. Acad. Sci. USA **97:**7078–7083. http://dx.doi.org/10.1073/pnas.97.13.7078.
22. **Marie CS, Verkerke HP, Paul SN, Mackey AJ, Petri WA.** 2012. Leptin protects host cells from Entamoeba histolytica cytotoxicity by a STAT3-dependent mechanism. Infect. Immun. **80:**1934–1943. http://dx.doi.org/10.1128/IAI.06140-11.
23. **Michalek RD, Rathmell JC, Michalek RD, Rathmell JC.** 2010. The metabolic life and times of a T-cell. Immunol. Rev. **236:**190–202. http://dx.doi.org/10.1111/j.1600-065X.2010.00911.x.
24. **Niiya T, Akbar SM, Yoshida O, Miyake T, Matsuura B, Murakami H, Abe M, Hiasa Y, Onji M.** 2007. Impaired dendritic cell function resulting from chronic undernutrition disrupts the antigen-specific immune response in mice. J. Nutr. **137:**671–675.
25. **Zhu S, Regev D, Watanabe M, Hickman D, Moussatche N, Jesus DM, Kahan SM, Napthine S, Brierley I, Hunter RN, III, Devabhaktuni D, Jones MK, Karst SM.** 2013. Identification of immune and viral correlates of norovirus protective immunity through comparative study of intra-cluster norovirus strains. PLoS Pathog. **9:**e1003592. http://dx.doi.org/10.1371/journal.ppat.1003592.
26. **Prasad BV, Hardy ME, Dokland T, Bella J, Rossmann MG, Estes MK.** 1999. X-ray crystallographic structure of the Norwalk virus capsid. Science **286:**287–290. http://dx.doi.org/10.1126/science.286.5438.287.
27. **Debbink K, Lindesmith LC, Donaldson EF, Costantini V, Beltramello M, Corti D, Swanstrom J, Lanzavecchia A, Vinjé J, Baric RS.** 2013. Emergence of new pandemic GII.4 Sydney norovirus strain correlates with escape from herd immunity. J. Infect. Dis. **208:**1877–1887. http://dx.doi.org/10.1093/infdis/jit370.
28. **Strong DW, Thackray LB, Smith TJ, Virgin HW.** 2012. Protruding domain of capsid protein is necessary and sufficient to determine murine norovirus replication and pathogenesis *in vivo*. J. Virol. **86:**2950–2958. http://dx.doi.org/10.1128/JVI.07038-11.
29. **Bailey D, Thackray LB, Goodfellow IG.** 2008. A single amino acid substitution in the murine norovirus capsid protein is sufficient for attenuation *in vivo*. J. Virol. **82:**7725–7728. http://dx.doi.org/10.1128/JVI.00237-08.
30. **De Filippo C, Cavalieri D, Di Paola M, Ramazzotti M, Poullet JB, Massart S, Collini S, Pieraccini G, Lionetti P.** 2010. Impact of diet in shaping gut microbiota revealed by a comparative study in children from Europe and rural Africa. Proc. Natl. Acad. Sci. USA **107:**14691–14696. http://dx.doi.org/10.1073/pnas.1005963107.
31. **Muegge BD, Kuczynski J, Knights D, Clemente JC, González A, Fontana L, Henrissat B, Knight R, Gordon JI.** 2011. Diet drives convergence in gut microbiome functions across mammalian phylogeny and within humans. Science **332:**970–974. http://dx.doi.org/10.1126/science.1198719.
32. **Wu GD, Chen J, Hoffmann C, Bittinger K, Chen YY, Keilbaugh SA, Bewtra M, Knights D, Walters WA, Knight R, Sinha R, Gilroy E, Gupta K, Baldassano R, Nessel L, Li H, Bushman FD, Lewis JD.** 2011. Linking long-term dietary patterns with gut microbial enterotypes. Science **334:** 105–108. http://dx.doi.org/10.1126/science.1208344.
33. **Turnbaugh PJ, Ridaura VK, Faith JJ, Rey FE, Knight R, Gordan JI.** 2009. The effect of diet on the human gut microbiome: a metagenomic analysis in humanized gnotobiotic mice. Sci. Transl. Med. **1:**–6ra14. http://dx.doi.org/10.1126/scitranslmed.3000322 6ra14.
34. **Abt MC, Artis D.** 2009. The intestinal microbiota in health and disease: the influence of microbial products on immune cell homeostasis. Curr. Opin. Gastroenterol. **25:**496–502. http://dx.doi.org/10.1097/MOG.0b013e328331b6b4.
35. **Gaboriau-Routhiau V, Rakotobe S, Lécuyer E, Mulder I, Lan A, Bridonneau C, Rochet V, Pisi A, De Paepe M, Brandi G, Eberl G, Snel J, Kelly D, Cerf-Bensussan N.** 2009. The key role of segmented filamentous bacteria in the coordinated maturation of gut helper T cell responses. Immunity **31:**677–689. http://dx.doi.org/10.1016/j.immuni.2009.08.020.
36. **Kau AL, Ahern PP, Griffin NW, Goodman AL, Gordon JI.** 2011. Human nutrition, the gut microbiome and the immune system. Nature **474:** 327–336. http://dx.doi.org/10.1038/nature10213.
37. **Kane M, Case LK, Kopaskie K, Kozlova A, MacDearmid C, Chervonsky AV, Golovkina TV.** 2011. Successful transmission of a retrovirus depends on the commensal microbiota. Science **334:**245–249. http://dx.doi.org/10.1126/science.1210718.
38. **Kuss SK, Best GT, Etheredge CA, Pruijssers AJ, Frierson JM, Hooper LV, Dermody TS, Pfeiffer JK.** 2011. Intestinal microbiota promote enteric virus replication and systemic pathogenesis. Science **334:**249–252. http://dx.doi.org/10.1126/science.1211057.
39. **Ma C, Wu X, Nawaz M, Li J, Yu P, Moore JE, Xu J.** 2011. Molecular characterization of fecal microbiota in patients with viral diarrhea. Curr. Microbiol. **63:**259–266. http://dx.doi.org/10.1007/s00284-011-9972-7.
40. **Nelson AM, Walk ST, Taube S, Taniuchi M, Houpt ER, Wobus CE, Young VB.** 2012. Disruption of the human gut microbiota following norovirus infection. PLoS ONE **7:**e48224. http://dx.doi.org/10.1371/journal.pone.0048224.
41. **Al-Ali RM, Chehadeh W, Hamze M, Dabboussi F, Hlais S, Mallat H.** 2011. First description of gastroenteritis viruses in Lebanese children: a

pilot study. J. Infect Public. Health **4:**59–64. http://dx.doi.org/10.1016/j.jiph.2011.01.002
42. **Jakab F, Németh V, Oldal M, Varga L, Nyul Z, Oldal M, Mitchell DK, Matson DO, Oldal M, Szucs G, Oldal M.** 2010. Epidemiological and clinical characterization of norovirus infections among hospitalized children in Baranya County, Hungary. J. Clin. Virol. **49:**75–76. http://dx.doi.org/10.1016/j.jcv.2010.06.010
43. **Kaplan NM, Kirby A, Abd-Eldayem SA, Dove W, Nakagomi T, Nakagomi O, Cunliffe NA.** 2011. Detection and molecular characterisation of rotavirus and norovirus infections in Jordanian children with acute gastroenteritis. Arch. Virol. **156:**1477–1480. http://dx.doi.org/10.1007/s00705-011-0996-x.
44. **Kirby A, Al-Eryani A, Al-Sonboli N, Hafiz T, Beyer M, Al-Aghbari N, Al-Moheri N, Dove W, Cunliffe NA, Cuevas LE.** 2011. Rotavirus and norovirus infections in children in Sana'a, Yemen. Trop. Med. Int. Health **16:**680–684. http://dx.doi.org/10.1111/j.1365-3156.2011.02756.x.
45. **Moyo SJ, Gro N, Matee MI, Kitundu J, Myrmel H, Mylvaganam H, Maselle SY, Langeland N.** 2011. Age specific aetiological agents of diarrhoea in hospitalized children aged less than five years in Dar es Salaam, Tanzania. BMC Pediatr. **11:**19. http://dx.doi.org/10.1186/1471-2431-11-19.
46. **Nataraju SM, Ganesh B, Das S, Chowdhury S, Nayak MK, Ghosh M, Chatterjee MK, Sarkar U, Mitra U, Bhattacharya MK, Arora R, Kobayashi N, Krishnan T.** 2010. Emergence of noroviruses homologous to strains reported from Djibouti (horn of Africa), Brazil, Italy, Japan and USA among children in Kolkata, India. Eur. Rev. Med. Pharmacol. Sci. **14:**789–794.
47. **O'Ryan ML, Peña A, Vergara R, Díaz J, Mamani N, Cortés H, Lucero Y, Vidal R, Osorio G, Santolaya ME, Hermosilla G, Prado VJ.** 2010. Prospective characterization of norovirus compared with rotavirus acute diarrhea episodes in Chilean Children. Pediatr. Infect. Dis. J. **29:**855–859. http://dx.doi.org/10.1097/INF.0b013e3181e8b346.
48. **Ozkul AA, Kocazeybek BS, Turan N, Reuter G, Bostan K, Yilmaz A, Altan E, Uyunmaz G, Karaköse AR, Muratoglu K, Elevli M, Helps CR, Yilmaz H.** 2011. Frequency and phylogeny of norovirus in diarrheic children in Istanbul, Turkey. J. Clin. Virol. **51:**160–164. http://dx.doi.org/10.1016/j.jcv.2011.03.004
49. **Rahouma A, Klena JD, Krema Z, Abobker AA, Treesh K, Franka E, Abusnena O, Shaheen HI, El Mohammady H, Abudher A, Ghenghesh KS.** 2011. Enteric pathogens associated with childhood diarrhea in Tripoli-Libya. Am. J. Trop. Med. Hyg. **84:**886–891. http://dx.doi.org/10.4269/ajtmh.2011.11-0116.
50. **Tamura T, Nishikawa M, Anh DD, Suzuki H.** 2010. Molecular epidemiological study of rotavirus and norovirus infections among children with acute gastroenteritis in Nha Trang. Vietnam, December 2005-2006. Jpn. J. Infect. Dis. **63:**405–411.
51. **Thongprachum A, Khamrin P, Chaimongkol N, Malasao R, Okitsu S, Mizuguchi M, Maneekarn N, Ushijima H.** 2010. Evaluation of an immunochromatography method for rapid detection of noroviruses in clinical specimens in Thailand. J. Med. Virol. **82:**2106–2109. http://dx.doi.org/10.1002/jmv.21916.
52. **Zhang S, Chen TH, Wang J, Dong C, Pan J, Moe C, Chen W, Yang L, Wang X, Tang H, Li X, Liu P.** 2011. Symptomatic and asymptomatic infections of rotavirus, norovirus, and adenovirus among hospitalized children in Xi'an, China. J. Med. Virol. **83:**1476–1484. http://dx.doi.org/10.1002/jmv.22108.
53. **Thackray LB, Wobus CE, Chachu KA, Liu B, Alegre ER, Henderson KS, Kelley ST, Virgin HW.** 2007. Murine noroviruses comprising a single genogroup exhibit biological diversity despite limited sequence divergence. J. Virol. **81:**10460–10473. http://dx.doi.org/10.1128/JVI.00783-07.
54. **Von Bubnoff A.** 2011. A gut response to vaccines. IAVI Rep. **15:**12–14.
55. **Chandra RK.** 1983. Nutrition, immunity, and infection: present knowledge and future directions. Lancet **i:**688–691.
56. **Fillol F, Sarr JB, Boulanger D, Cisse B, Sokhna C, Riveau G, Simondon KB, Remoué F.** 2009. Impact of child malnutrition on the specific anti-Plasmodium falciparum antibody response. Malar. J. **8:**116. http://dx.doi.org/10.1186/1475-2875-8-116.
57. **Ishikawa LL, França TG, Chiuso-Minicucci F, Zorzella-Pezavento SF, Marra NM, Pereira PC, Silva CL, Sartori A.** 2009. Dietary restriction abrogates antibody production induced by a DNA vaccine encoding the mycobacterial 65 kDa heat shock protein. Genet. Vaccines Ther. **7:**11. http://dx.doi.org/10.1186/1479-0556-7-11.
58. **Kizito D, Tweyongyere R, Namatovu A, Webb EL, Muhangi L, Lule SA, Bukenya H, Cose S, Elliott AM.** 2013. Factors affecting the infant antibody response to measles immunisation in Entebbe-Uganda. BMC Public Health **13:**619. http://dx.doi.org/10.1186/1471-2458-13-619.
59. **Taylor AK, Cao W, Vora KP, De La Cruz J, Shieh WJ, Zaki SR, Katz JM, Sambhara S, Gangappa S.** 2013. Protein energy malnutrition decreases immunity and increases susceptibility to influenza infection in mice. J. Infect. Dis. **207:**501–510. http://dx.doi.org/10.1093/infdis/jis527.
60. **Guzman MG, Alvarez M, Halstead SB.** 2013. Secondary infection as a risk factor for dengue hemorrhagic fever/dengue shock syndrome: an historical perspective and role of antibody-dependent enhancement of infection. Arch. Virol. **158:**1445–1459. http://dx.doi.org/10.1007/s00705-013-1645-3.
61. **Grenfell BT, Pybus OG, Gog JR, Wood JL, Daly JM, Mumford JA, Holmes EC.** 2004. Unifying the epidemiological and evolutionary dynamics of pathogens. Science **303:**327–332. http://dx.doi.org/10.1126/science.1090727.
62. **Siebenga JJ, Beersma MF, Vennema H, van Biezen P, Hartwig NJ, Koopmans M.** 2008. High prevalence of prolonged norovirus shedding and illness among hospitalized patients: a model for *in vivo* molecular evolution. J. Infect. Dis. **198:**994–1001. http://dx.doi.org/10.1086/591627.
63. **Wobus CE, Karst SM, Thackray LB, Chang KO, Sosnovtsev SV, Belliot G, Krug A, Mackenzie JM, Green KY, Virgin HW.** 2004. Replication of norovirus in cell culture reveals a tropism for dendritic cells and macrophages. PLoS Biol. **2:**e432. http://dx.doi.org/10.1371/journal.pbio.0020432.
64. **Monira S, Nakamura S, Endtz HP, Cravioto A, Izutsu K, Watanabe H, Alam NH, Nakaya T, Horii T, Iida T, Alam M.** 2011. Gut microbiota of healthy and malnourished children in Bangladesh. Front. Evol. **2:**228. http://dx.doi.org/10.3389/fmicb.2011.00228.
65. **Ley RE, Bäckhed F, Turnbaugh P, Lozupone CA, Knight RD, Gordon JI.** 2005. Obesity alters gut microbial ecology. Proc. Natl. Acad. Sci. U. S. A. **102:**11070–11075. http://dx.doi.org/10.1073/pnas.0504978102.
66. **Turnbaugh PJ, Hamady M, Yatsunenko T, Cantarel BL, Duncan A, Ley RE, Sogin ML, Jones WJ, Roe BA, Affourtit JP, Egholm M, Henrissat B, Heath AC, Knight R, Gordon JI.** 2009. A core gut microbiome in obese and lean twins. Nature **457:**480–484. http://dx.doi.org/10.1038/nature07540.
67. **Ng KM, Ferreyra JA, Higginbottom SK, Lynch JB, Kashyap PC, Gopinath S, Naidu N, Choudhury B, Weimer BC, Monack DM, Sonnenburg JL.** 2013. Microbiota-liberated host sugars facilitate post-antibiotic expansion of enteric pathogens. Nature **502:**96–99. http://www.nature.com/nature/journal/vaop/ncurrent/full/nature12503.html#supplementary-information.
68. **Arumugam M, Raes J, Pelletier E, Le Paslier D, Yamada T, Mende DR, Fernandes GR, Tap J, Bruls T, Batto JM, Bertalan M, Borruel N, Casellas F, Fernandez L, Gautier L, Hansen T, Hattori M, Hayashi T, Kleerebezem M, Kurokawa K, Leclerc M, Levenez F, Manichanh C, Nielsen HB, Nielsen T, Pons N, Poulain J, Qin J, Sicheritz-Ponten T, Tims S, Torrents D, Ugarte E, Zoetendal EG, Wang J, Guarner F, Pedersen O, de Vos WM, Brunak S, Doré J, MetaHIT Consortium, Antolín M, Artiguenave F, Blottiere HM, Almeida M, Brechot C, Cara C, Chervaux C, Cultrone A, Delorme C, Denariaz G, et al.** 2011. Enterotypes of the human gut microbiome. Nature **473:**174–180. http://dx.doi.org/10.1038/nature09944.
69. **Agus SG, Dolin R, Wyatt RG, Tousimis AJ, Northrup RS.** 1973 Acute infectious nonbacterial gastroenteritis: intestinal histopathology. Histologic and enzymatic alterations during illness produced by the Norwalk agent in man. Ann. Intern. Med. **79:**18–25.
70. **Round JL, Mazmanian SK.** 2010. Inducible Foxp3+ regulatory T-cell development by a commensal bacterium of the intestinal microbiota. Proc. Natl. Acad. Sci. USA **107:**12204–12209. http://dx.doi.org/10.1073/pnas.0909122107.
71. **Mazmanian SK, Round JL, Kasper DL.** 2008. A microbial symbiosis factor prevents intestinal inflammatory disease. Nature **453:**620–625. http://dx.doi.org/10.1038/nature07008.
72. **Troy EB, Kasper DL.** 2010. Beneficial effects of Bacteroides fragilis polysaccharides on the immune system. Front. Biosci. **15:**25–34. http://dx.doi.org/10.2741/3603.
73. **Gauffin Cano P, Santacruz A, Moya Á, Sanz Y.** 2012. Bacteroides uniformis CECT 7771 ameliorates metabolic and immunological dysfunction in mice with high-fat-diet induced obesity. PLoS One **7:**e41079. http://dx.doi.org/10.1371/journal.pone.0041079.
74. **Tamura K, Peterson D, Peterson N, Stecher G, Nei M, Kumar S.** 2011.

MEGA5: molecular evolutionary genetics analysis using maximum likelihood, evolutionary distance, and maximum parsimony methods. Mol. Biol. Evol. **28:**2731–2739. http://dx.doi.org/10.1093/molbev/msr121.

75. **Mai V, Greenwald B, Morris JG, Raufman JP, Stine OC.** 2006. Effect of bowel preparation and colonoscopy on post-procedure intestinal microbiota composition. Gut **55:**1822–1823. http://dx.doi.org/10.1136/gut.2006.108266.
76. **Cai Y, Sun Y.** 2011. ESPRIT-Tree: hierarchical clustering analysis of millions of 16S rRNA pyrosequences in quasilinear computational time. Nucleic Acids Res. **39:**e95. http://dx.doi.org/10.1093/nar/gkr349.
77. **Sun Y, Cai Y, Liu L, Yu F, Farrell ML, McKendree W, Farmerie W.** 2009. ESPRIT: estimating species richness using large collections of 16S rRNA pyrosequences. Nucleic Acids Res. **37:**e76. http://dx.doi.org/10.1093/nar/gkp285.
78. **Caporaso JG, Kuczynski J, Stombaugh J, Bittinger K, Bushman FD, Costello EK, Fierer N, Peña AG, Goodrich JK, Gordon JI, Huttley GA, Kelley ST, Knights D, Koenig JE, Ley RE, Lozupone CA, McDonald D, Muegge BD, Pirrung M, Reeder J, Sevinsky JR, Turnbaugh PJ, Walters WA, Widmann J, Yatsunenko T, Zaneveld J, Knight R.** 2010. QIIME allows analysis of high-throughput community sequencing data. Nat. Methods **7:**335–336. http://dx.doi.org/10.1038/nmeth.f.303.
79. **Lozupone C, Knight R.** 2005. UniFrac: a new phylogenetic method for comparing microbial communities. Appl. Environ. Microbiol. **71:**8228–8235. http://dx.doi.org/10.1128/AEM.71.12.8228-8235.2005.